Supporting Information

for the paper

Synthesis and characterisation of the complete series of B−N analogues of triptycene

Ömer Seven, Sebastian Popp, Michael Bolte, Hans-Wolfram Lerner, Matthias Wagner*

Institut für Anorganische Chemie, J.W. Goethe-Universität Frankfurt, Max-von-Laue-Strasse 7, D-60438 Frankfurt (Main), Germany.
E-mail: Matthias.Wagner@chemie.uni-frankfurt.de

Content:

1) Syntheses of 3c, 3d, 3e, K[8] (R = *p*-$Me_3SiC_6H_4$; *p*-IC_6H_4), 14c and 14d

Synthesis of 3c. A Schlenk flask was charged with Li_2[**7**]·OEt_2 (25 mg, 0.13 mmol) and 3,5-dimethylpyrazole (25 mg, 0.26 mmol). Et_2O (15 mL) was added at rt with stirring, whereupon vigorous gas evolution (H_2) was observed, which lasted for approximately 2 min. After 30 min, neat Me_3SiCl (0.1 mL, 0.08 g, 0.8 mmol) was added to the colourless solution to give a white suspension. Stirring was continued for 12 h, the formed LiCl was removed by filtration and the filtrate was evaporated under vacuum to yield a colourless solid. Single crystals were grown by gas-phase diffusion of cyclohexane into a solution of **3c** in C_6H_6. Yield: 27 mg (71%). ^{1}H NMR (400.1 MHz, C_6D_6): δ = 7.99-7.93 (2 H, m, H-3,6), 7.32-7.28 (2 H, m, H-4,5), 5.19 (2 H, s, pzH-4), 4.70 (2 H, br q, BH), 2.06 (12 H, s, Me); ^{13}C{^{1}H} NMR (75.4 MHz, C_6D_6): δ = 143.0 (pzC-3,5), 130.3 (C-3,6), 126.0 (C-4,5), 105.1 (pzC-4), 11.4 (Me), n.o. (CB); ^{11}B NMR (96.3 MHz, C_6D_6): δ = −7.0 (d, $^1J_{B,H}$ = 98 Hz); ^{11}B{^{1}H} NMR (96.3 MHz, C_6D_6): δ = −7.0 ($h_{1/2}$ = 120 Hz); MS (ESI$^+$): *m/z* 291.3 ([M + H]$^+$, 100%); HRMS (MALDI-TOF): *m/z* = 291.19474 ([M + H]$^+$, calcd 291.19468).

Synthesis of 3d. A solution of 3,5-di(*tert*-butyl)pyrazole (47 mg, 0.26 mmol) in Et_2O (10 mL) was added dropwise with stirring at rt to a solution of Li_2[**7**]·OEt_2 (25 mg, 0.13 mmol) in Et_2O (10 mL); the reaction proceeds with evolution of H_2. After 30 min, neat Me_3SiCl (0.1 mL, 0.08 g, 0.8 mmol) was added to the clear colourless solution to give a white suspension. Stirring was continued for 12 h, the formed LiCl was removed by filtration and the filtrate was evaporated under vacuum to yield a colourless solid. Single crystals were obtained as colourless plates by slow evaporation of a solution of **3d** in Et_2O. Yield: 51 mg (85%). ^{1}H NMR (500.2 MHz, C_6D_6): δ = 7.81-7.77 (2 H, m, H-3,6), 7.27-7.23 (2 H, m, H-4,5), 5.88 (2 H, s, pzH-4), 5.32 (2 H, br, BH), 1.44 (36 H, s, *t*Bu); ^{13}C{^{1}H} NMR (125.8 MHz, C_6D_6): δ = 156.8 (pzC-3,5), 129.4 (C-3,6), 125.7 (C-4,5), 102.1 (pzC-4), 32.3 ($C(CH_3)_3$), 30.6 (CH_3), n.o. (CB); ^{11}B NMR (160.5 MHz, C_6D_6): δ = −4.0 ($h_{1/2}$ = 350 Hz); MS (ESI$^+$): *m/z* 459.5 ([M + H]$^+$, 100%); HRMS (MALDI-TOF): *m/z* = 459.38367 ([M + H]$^+$, calcd 459.38248).

Synthesis of 3e. A Schlenk flask was charged with Li_2[**7**]·OEt_2 (40 mg, 0.21 mmol) and 3,5-bis(trifluoromethyl)pyrazole (85 mg, 0.42 mmol). Et_2O (10 mL) was added at rt with stirring, whereupon vigorous gas evolution (H_2) was observed, which lasted for approximately 2 min. After 30 min, neat Me_3SiCl (0.1 mL, 0.08 g, 0.8 mmol) was added to the colourless solution to give a white suspension. Stirring was continued for 15 h, the formed LiCl was removed by

filtration and the filtrate was evaporated under vacuum to yield a colourless solid. Single crystals were obtained as colourless plates by slow evaporation of a solution of **3e** in C_6H_6. Yield: 80 mg (76%). (Found: C, 37.74; H, 1.59; N, 10.85. Calc. for $C_{16}H_8B_2F_{12}N_4$ [505.86]: C, 37.99; H, 1.59; N, 11.08%); ^{1}H NMR (500.2 MHz, C_6D_6): δ = 7.77-7.74 (2 H, m, H-3,6), 7.14-7.10 (2 H, m, H-4,5), 5.63 (2 H, s, pzH-4), 4.93 (2 H, br, BH); ^{13}C{^{1}H} NMR (75.4 MHz, C_6D_6): δ = 137.7 (q, $^2J_{C,F}$ = 42.2 Hz, pzC-3,5), 131.4 (C-3,6), 127.9 (C-4,5) 118.8 (q, $^1J_{C,F}$ = 270.8 Hz, CF_3), 106.4 (pzC-4), n.o. (CB); ^{11}B{^{1}H} NMR (160.5 MHz, C_6D_6): δ = −3.7 ($h_{1/2}$ = 290 Hz).

Syntheses of K[8] (R = *p*-Me$_3$SiC$_6$H$_4$; *p*-IC$_6$H$_4$). The potassium tris(pyrazol-1-yl)borate salts K[HBpz$_3$][1S] and K[*p*-BrC$_6$H$_4$Bpz$_3$][2S] were synthesised according to published procedures. The syntheses of K[*p*-Me$_3$SiC$_6$H$_4$Bpz$_3$] and K[*p*-IC$_6$H$_4$Bpz$_3$] were performed as outlined in Scheme 1S; detailed protocols are given below. The sodium salt Na[*p*-IC$_6$H$_4$Bpz$_3$] is literature known.[3S]

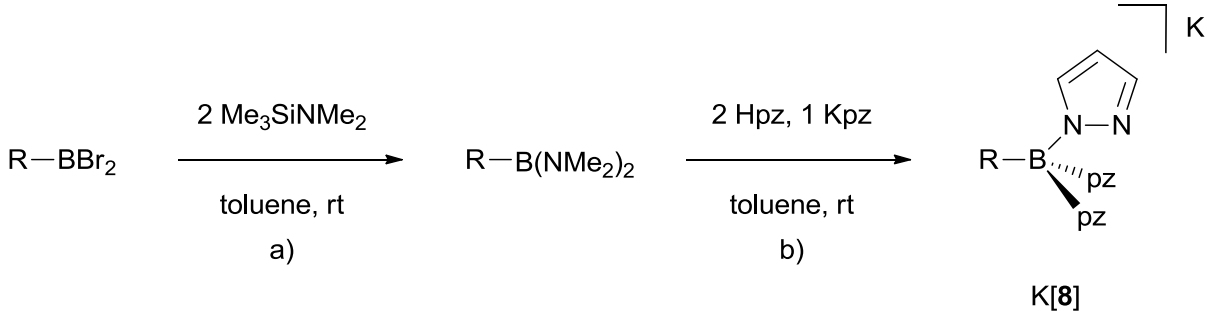

K[**8**]

Scheme 1S: Syntheses of K[**8**] (R = *p*-Me$_3$SiC$_6$H$_4$ or *p*-IC$_6$H$_4$; Hpz = pyrazole).

Step a)

Synthesis of *p*-Me$_3$SiC$_6$H$_4$B(NMe$_2$)$_2$. Neat Me$_3$SiNMe$_2$ (6.9 mL, 5.1 g, 44 mmol) was added dropwise with stirring at rt to a solution of *p*-Me$_3$SiC$_6$H$_4$BBr$_2$[4S] (7.0 g, 22 mmol) in toluene (10 mL); stirring was continued for 2.5 h. All volatiles were removed under reduced pressure to afford *p*-Me$_3$SiC$_6$H$_4$B(NMe$_2$)$_2$ as a brown oil, which was used without further purification. Yield: 3.8 g (70%). ^{1}H NMR (400.1 MHz, C_6D_6): δ = 7.59 (2 H, d, $^3J_{H,H}$ = 8.0 Hz, ArH), 7.51 (2 H, d, $^3J_{H,H}$ = 8.0 Hz, ArH), 2.61 (12 H, s, NMe$_2$), 0.27 (9 H, s, SiMe$_3$); ^{13}C{^{1}H} NMR (75.4 MHz, C_6D_6): δ = 139.3 (CSi), 133.4 (ArC), 133.0 (ArC), 41.2 (NMe$_2$), −0.9 (SiMe$_3$), n.o. (CB); ^{11}B NMR (128.4 MHz, C_6D_6): δ = 32.8 ($h_{1/2}$ = 240 Hz); ^{29}Si INEPT NMR (99.4 MHz, C_6D_6): δ = −4.9.

Synthesis of *p*-$IC_6H_4B(NMe_2)_2$. The compound was synthesised according to the protocol described above for *p*-$Me_3SiC_6H_4B(NMe_2)_2$ from Me_3SiNMe_2 (1.8 mL, 1.3 g, 11 mmol) and *p*-$IC_6H_4BBr_2$[3S] (2.1 g, 5.6 mmol). Yield: 1.6 g (94%). ^{1}H NMR (300.0 MHz, C_6D_6): δ = 7.61 (2 H, d, $^3J_{H,H}$ = 8.2 Hz, ArH), 6.95 (2 H, d, $^3J_{H,H}$ = 8.2 Hz, ArH), 2.48 (12 H, s, NMe_2); $^{13}C\{^1H\}$ NMR (75.4 MHz, C_6D_6): δ = 137.1 (ArC), 135.8 (ArC), 94.5 (CI), 40.9 (NMe_2), n.o. (CB); ^{11}B NMR (96.3 MHz, C_6D_6): δ = 32.3 ($h_{1/2}$ = 130 Hz).

Step b)

Synthesis of K[*p*-$Me_3SiC_6H_4Bpz_3$]. *p*-$Me_3SiC_6H_4B(NMe_2)_2$ (2.68 g, 10.8 mmol), Hpz (1.47 g, 21.6 mmol) and Kpz (1.15 g, 10.8 mmol) were suspended in toluene (20 mL). The suspension was stirred for 24 h at rt, whereupon the potassium tris(pyrazol-1-yl)borate gradually precipitated. The colourless precipitate was collected on a frit, washed with toluene (6 × 5 mL) and *n*-pentane (6 × 5 mL) and dried under reduced pressure. Yield: 3.5 g (81%). ^{1}H NMR (500.2 MHz, d_8-THF): δ = 7.43 (3 H, d, $^3J_{H,H}$ = 1.0 Hz, pzH-3 or pzH-5), 7.34 (3 H, d, $^3J_{H,H}$ = 2.0 Hz, pzH-3 or pzH-5), 7.32 (2 H, d, $^3J_{H,H}$ = 8.0 Hz, ArH), 6.93 (2 H, d, $^3J_{H,H}$ = 8.0 Hz, ArH), 5.99 (3 H, vtr, pzH-4), 0.23 (9 H, s, $SiMe_3$); $^{13}C\{^1H\}$ NMR (125.8 MHz, d_8-THF): δ = 139.4 (pzC-3 or pzC-5), 137.5 (CSi), 135.9 (pzC-3 or pzC-5), 134.5 (ArC), 132.4 (ArC), 103.0 (pzC-4), −0.8 ($SiMe_3$), n.o. (CB); $^{11}B\{^1H\}$ NMR (160.5 MHz, d_8-THF): δ = 1.7 ($h_{1/2}$ = 130 Hz); ^{29}Si INEPT NMR (99.4 MHz, d_8-THF): δ = −5.3; MS (ESI^-): *m/z* 361.3 ($[M - K]^-$, 100%); MS (ESI^+): *m/z* 439.3 ($[M + K]^+$, 100%).

Synthesis of K[*p*-$IC_6H_4Bpz_3$]. The compound was synthesised according to the protocol described above for K[*p*-$Me_3SiC_6H_4Bpz_3$] from *p*-$IC_6H_4B(NMe_2)_2$ (3.15 g, 10.4 mmol), Hpz (1.42 g, 20.9 mmol) and Kpz (1.11 g, 10.5 mmol). Yield: 4.1 g (87%). ^{1}H NMR (500.2 MHz, d_8-THF): δ = 7.47 (2 H, d, $^3J_{H,H}$ = 8.0 Hz, ArH), 7.44 (3 H, n.r., pzH-3 or pzH-5), 7.33 (3 H, d, $^3J_{H,H}$ = 2.0 Hz, pzH-3 or pzH-5), 6.70 (2 H, d, $^3J_{H,H}$ = 8.0 Hz, ArH), 6.00 (3 H, vtr, pzH-4); $^{13}C\{^1H\}$ NMR (125.8 MHz, d_8-THF): δ = 139.5 (pzC-3 or pzC-5), 137.3 (ArC), 136.4 (ArC), 135.8 (pzC-3 or pzC-5), 103.2 (pzC-4), 93.0 (CI), n.o. (CB); ^{11}B NMR (96.3 MHz, d_8-THF): δ = 1.5 ($h_{1/2}$ = 90 Hz).

The NMR data of K[*p*-$IC_6H_4Bpz_3$] are in agreement with those of Na[*p*-$IC_6H_4Bpz_3$].[3S]

1S S. Trofimenko, *J. Am. Chem. Soc.*, 1967, **89**, 3170−3177.

2S J. Zagermann, M. C. Kuchta, K. Merz and N. Metzler-Nolte, *Eur. J. Inorg. Chem.*, 2009, 5407−5412.

3S D. L. Reger, J. R. Gardinier, M. D. Smith, A. M. Shahin, G. J. Long, L. Rebbouh and F. Grandjean, *Inorg. Chem.*, 2005, **44**, 1852−1866.

4S D. Kaufmann, *Chem. Ber.*, 1987, **120**, 901−905.

Synthesis of 14c. A Schlenk flask was charged with Li_4[**13**]·3thf (50 mg, 0.13 mmol) and 3,5-dimethylpyrazole (51 mg, 0.53 mmol). Toluene (30 mL) was added at rt with stirring, whereupon a gas (H_2) evolved. After 10 min, neat Me_3SiCl (0.1 mL, 0.08 g, 0.8 mmol) was added to the colourless suspension and stirring was continued for 5 d. All insolubles were collected on a frit, washed with toluene (2 × 5 mL) and dried under vacuum to obtain a mixture of **14c** and LiCl. **14c** is insoluble in hexane, C_6H_6, toluene, and Et_2O; it is only sparingly soluble in THF, $CHCl_3$, and CH_2Cl_2. The solid mixture of **14c** and LiCl was washed with H_2O (2 × 5 mL) and pentane (2 × 5 mL) and dried under vacuum (12 h). Yield: 47 mg (70%). ^{1}H NMR (500.2 MHz, $CDCl_3$): δ = 7.70 (2 H, s, H-3,6), 5.51 (4 H, s, pzH-4), 4.30* (4 H, br, BH), 2.27 (24 H, s, Me); ^{13}C{^{1}H} NMR (125.8 MHz, $CDCl_3$): δ = 142.5 (pzC-3,5), 132.0 (C-3,6), 104.5 (pzC-4), 11.7 (Me), n.o. (CB); ^{11}B NMR (96.3 MHz, $CDCl_3$): δ = −7.0 (br, $h_{1/2}$ = 500 Hz); ^{11}B{^{1}H} NMR (96.3 MHz, $CDCl_3$): δ = −7.0 ($h_{1/2}$ = 400 Hz); MS (ESI$^+$): *m/z* 502.9 ([M + H]$^+$, 100%); HRMS (MALDI-TOF): *m/z* = 503.33414 ([M + H]$^+$, calcd 503.33683). *This signal sharpens upon ^{11}B decoupling.

Synthesis of 14d. A glass ampoule was charged with Li_4[**13**]·3thf (50 mg, 0.13 mmol), 3,5-di(*tert*-butyl)pyrazole (94 mg, 0.52 mmol), and toluene (20 mL). Neat Me_3SiCl (0.1 mL, 0.08 g, 0.8 mmol) was added to the colourless suspension. The ampoule was sealed under vacuum and stored at 80 °C for 7 d. The ampoule was opened at rt, all insolubles were collected on a frit, washed with toluene (2 × 5 mL), and dried under vacuum to obtain a mixture of **14d** and LiCl. **14d** is insoluble in hexane, C_6H_6, toluene, and Et_2O; it is only sparingly soluble in THF, $CHCl_3$, and CH_2Cl_2. The solid mixture of **14d** and LiCl was washed with H_2O (2 × 5 mL) and pentane (2 × 5 mL) and dried under vacuum (12 h). Yield: 77 mg (69%). ^{1}H NMR (500.2 MHz, $CDCl_3$): δ = 7.35 (2 H, s, H-3,6), 5.65 (4 H, s, pzH-4), 4.85* (4 H, br, BH), 1.41 (72 H, s, *t*Bu); ^{13}C{^{1}H} NMR (125.8 MHz, $CDCl_3$): δ = 155.5 (pzC-3,5), 130.1 (C-3,6), 100.9 (pzC-4), 32.1 (*C*$(CH_3)_3$), 30.6 (CH_3), n.o. (CB); ^{11}B{^{1}H} NMR (96.3 MHz, $CDCl_3$): δ = −3.5 ($h_{1/2}$ = 800 Hz); MS (ESI$^+$): *m/z* 845.5 ([M + Li]$^+$, 100%), *m/z* 839.5 ([M + H]$^+$, 71%); HRMS (MALDI-TOF): *m/z* = 838.70550 ([M]$^+$, calcd 838.70580). *This signal sharpens upon ^{11}B decoupling.

2) Plots of the $^{13}C\{^{1}H\}$ NMR spectra of 3a, 3c, 3d, [4a]Br, [4c]Br, [4e]Br, 14b, 14c and 14d

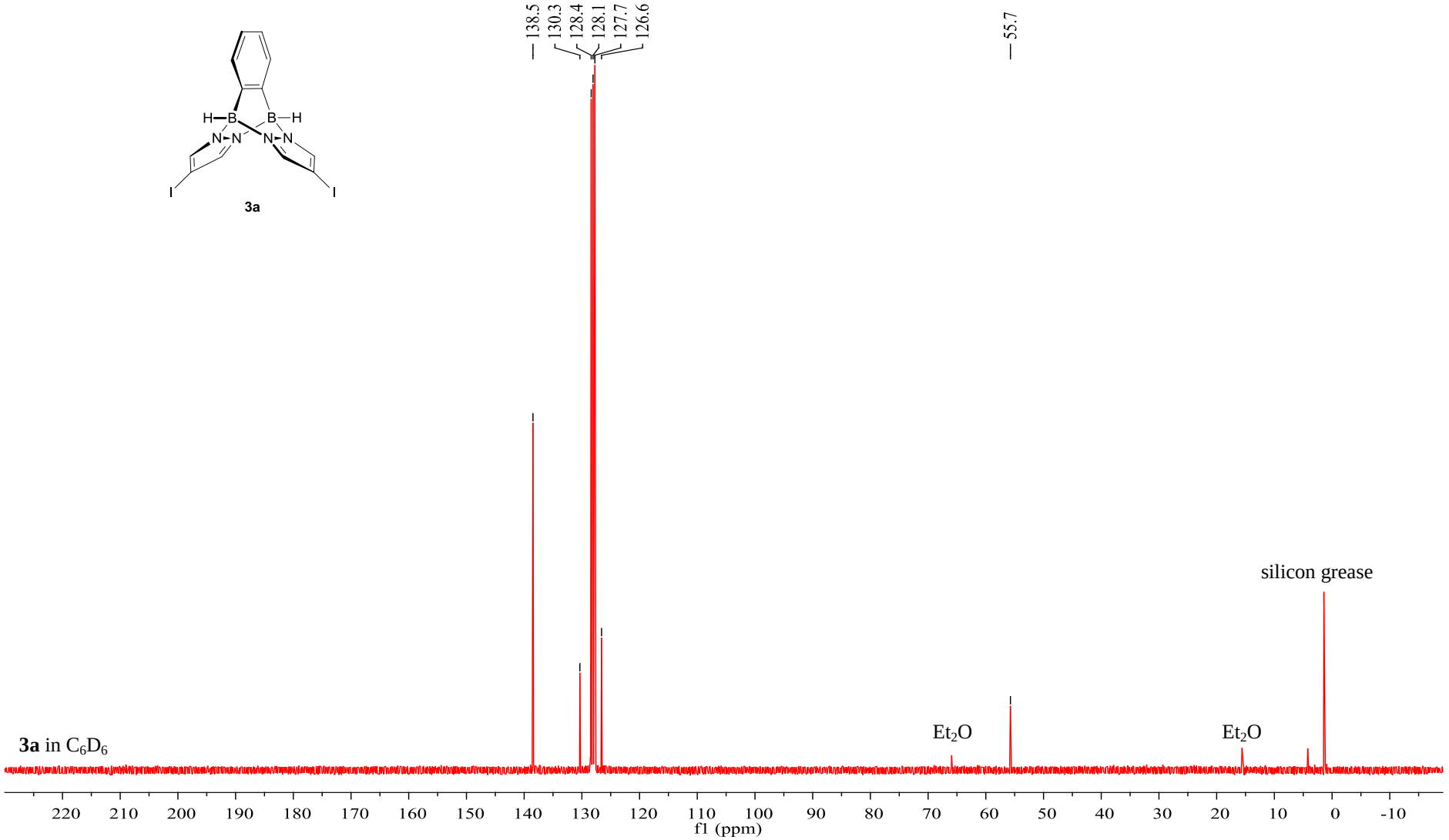

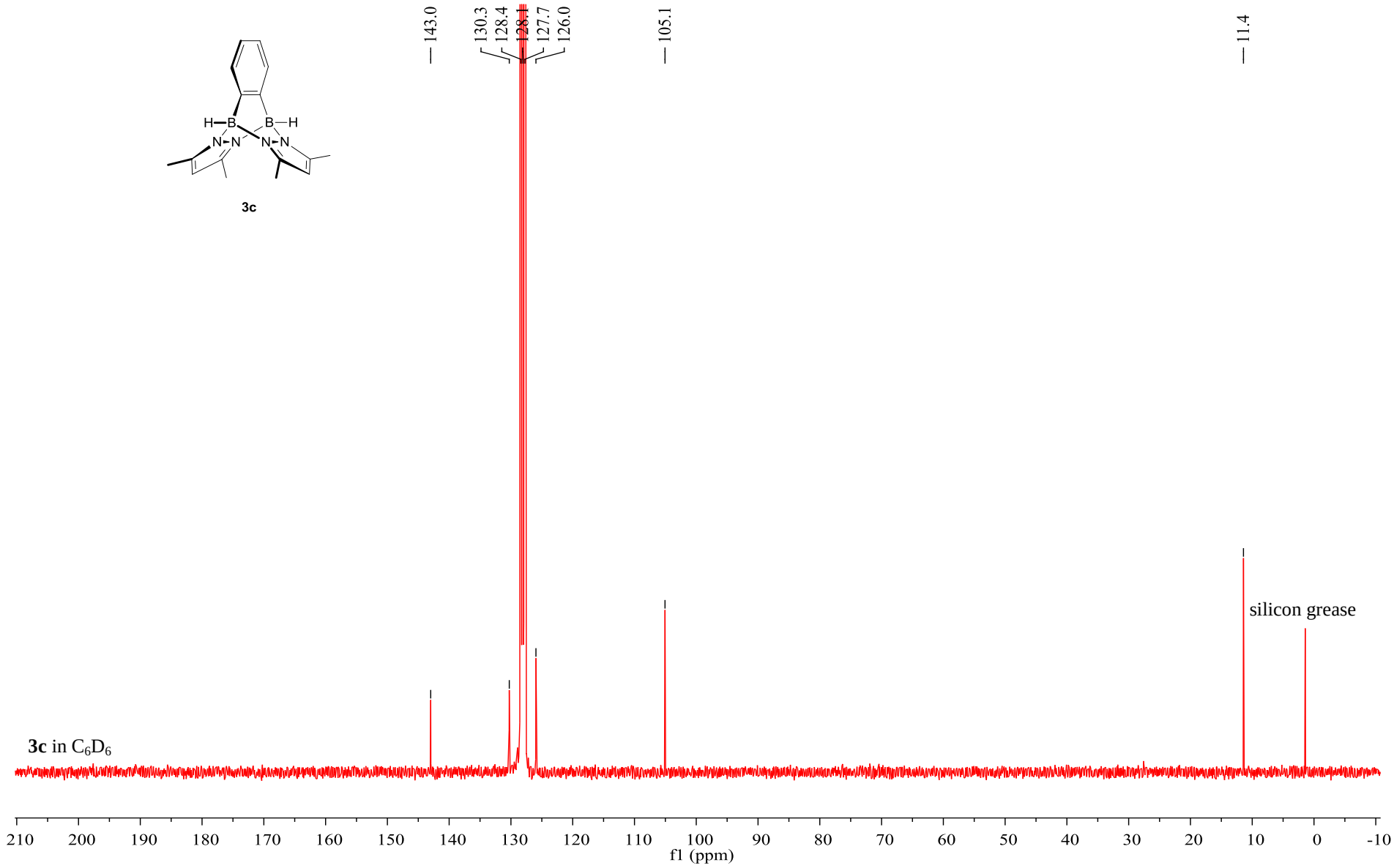
143.0
130.3
128.4
128.1
127.7
126.0
105.1
11.4
3c
silicon grease
3c in C6D6
210 200 190 180 170 160 150 140 130 120 110 100 90 80 70 60 50 40 30 20 10 0 -10
f1 (ppm)

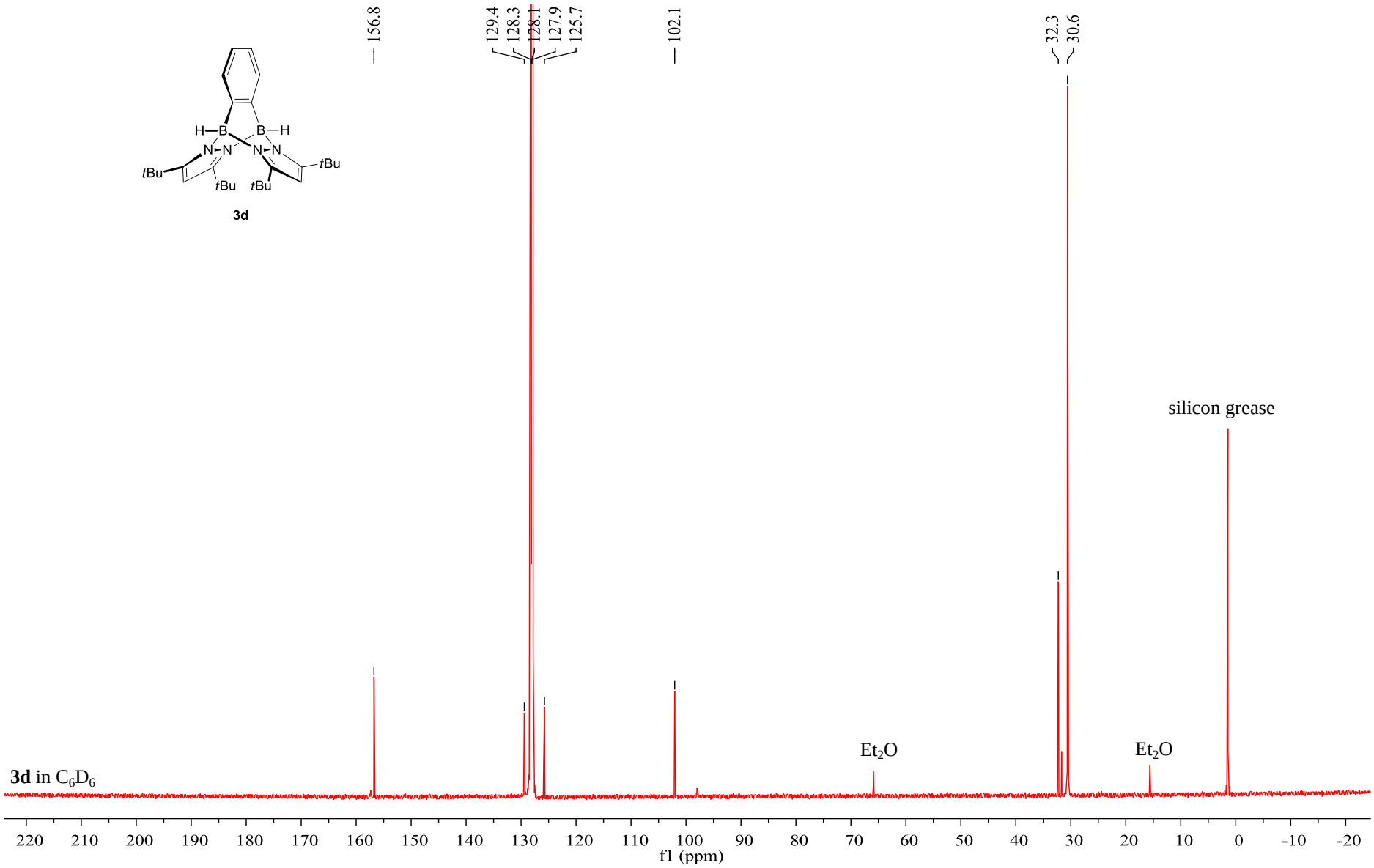
156.8
129.4
128.3
128.1
127.9
125.7
102.1
32.3
30.6
tBu
tBu
tBu
tBu
tBu
3d
silicon grease
Et2O
Et2O
3d in C6D6
220 210 200 190 180 170 160 150 140 130 120 110 100 90 80 70 60 50 40 30 20 10 0 -10 -20
f1 (ppm)

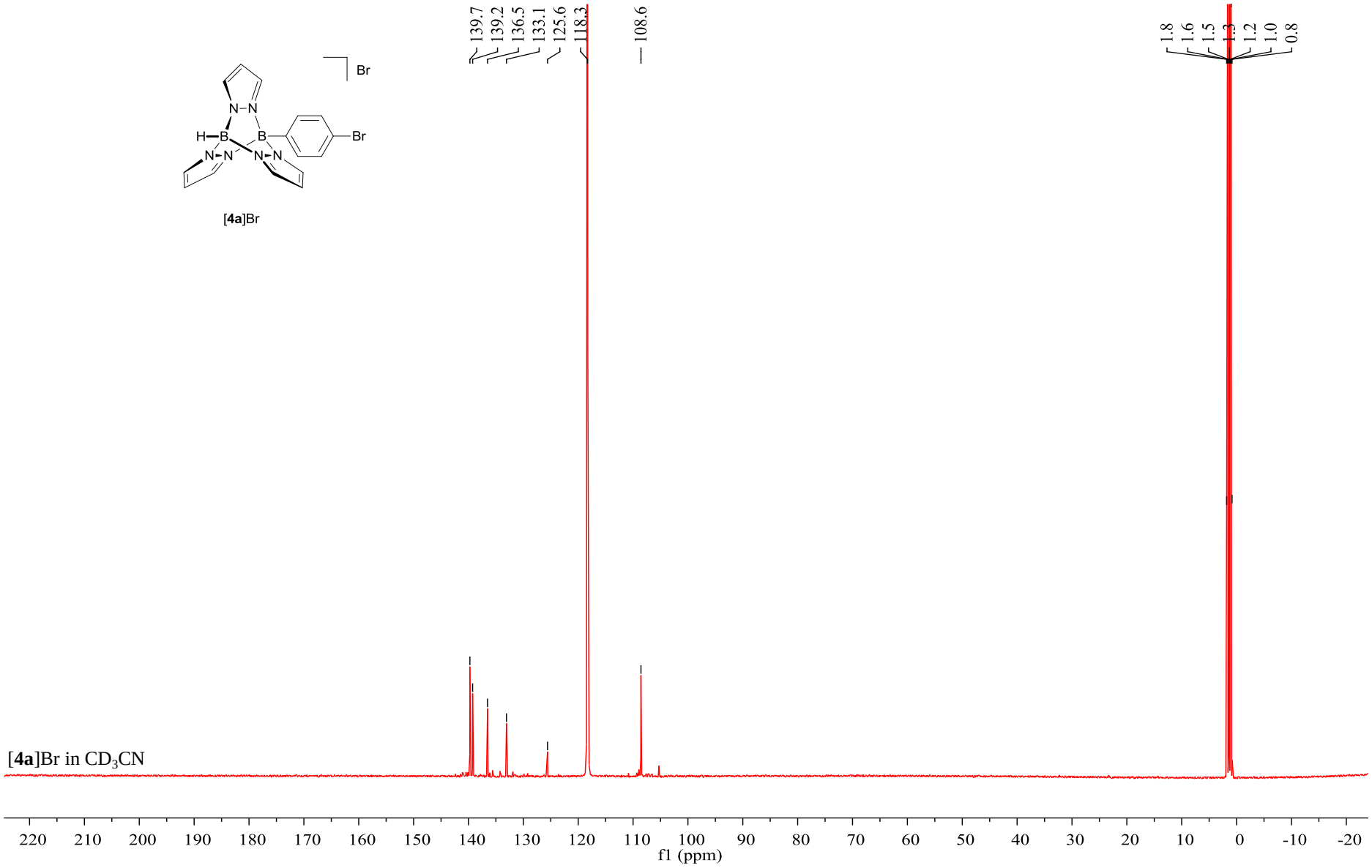
Br
N–N
H–B
B
Br
N–N
N–N
[4a]Br
139.7
139.2
136.5
133.1
125.6
118.3
108.6
1.8
1.6
1.5
1.3
1.2
1.0
0.8
[4a]Br in CD3CN
220 210 200 190 180 170 160 150 140 130 120 110 100 90 80 70 60 50 40 30 20 10 0 -10 -20
f1 (ppm)

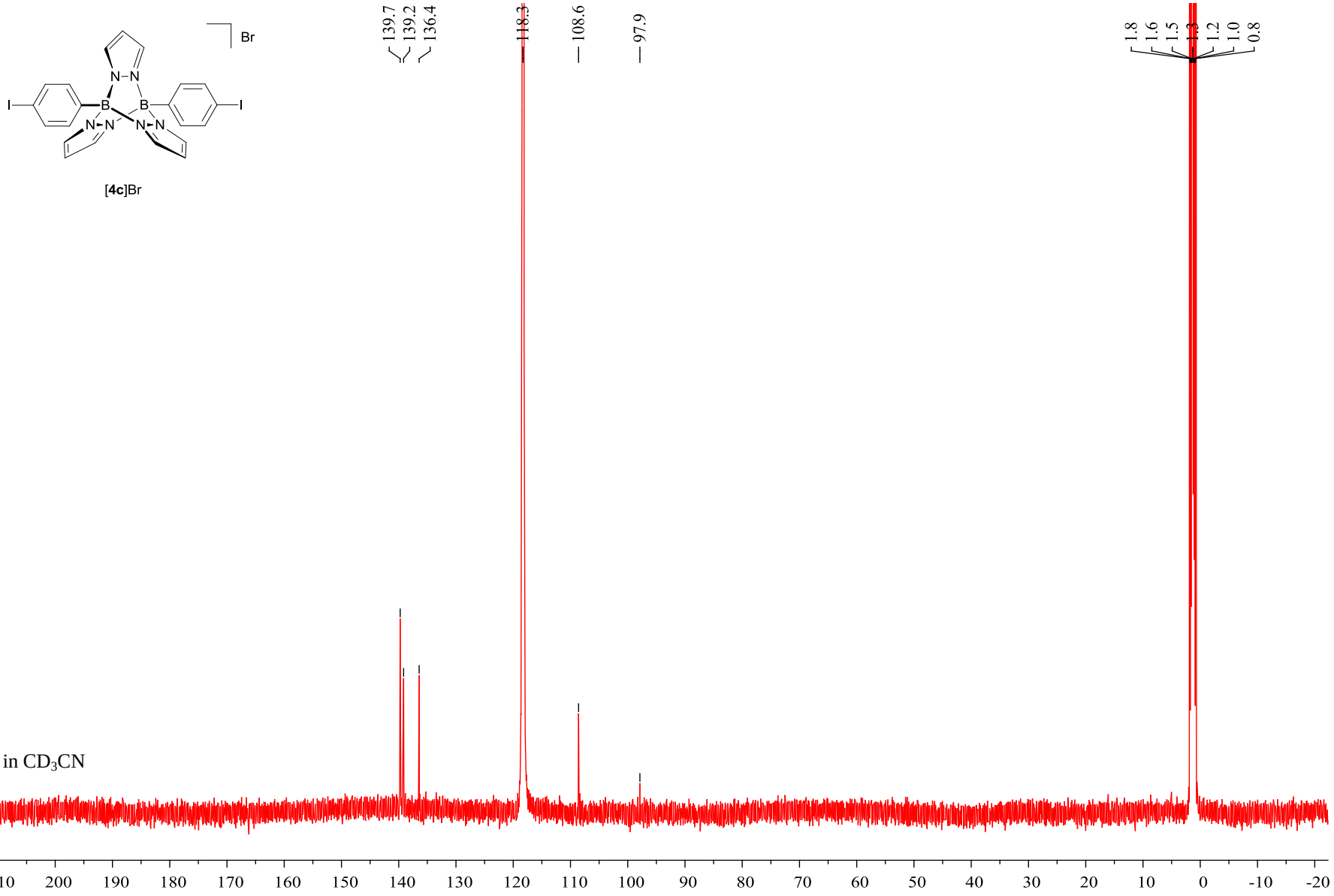
Br
I
I
N–N
B
B
N–N
N–N
[4c]Br
139.7
139.2
136.4
118.3
108.6
97.9
1.8
1.6
1.5
1.3
1.2
1.0
0.8
[4c]Br in CD3CN
220
210
200
190
180
170
160
150
140
130
120
110
100
90
80
70
60
50
40
30
20
10
0
-10
-20

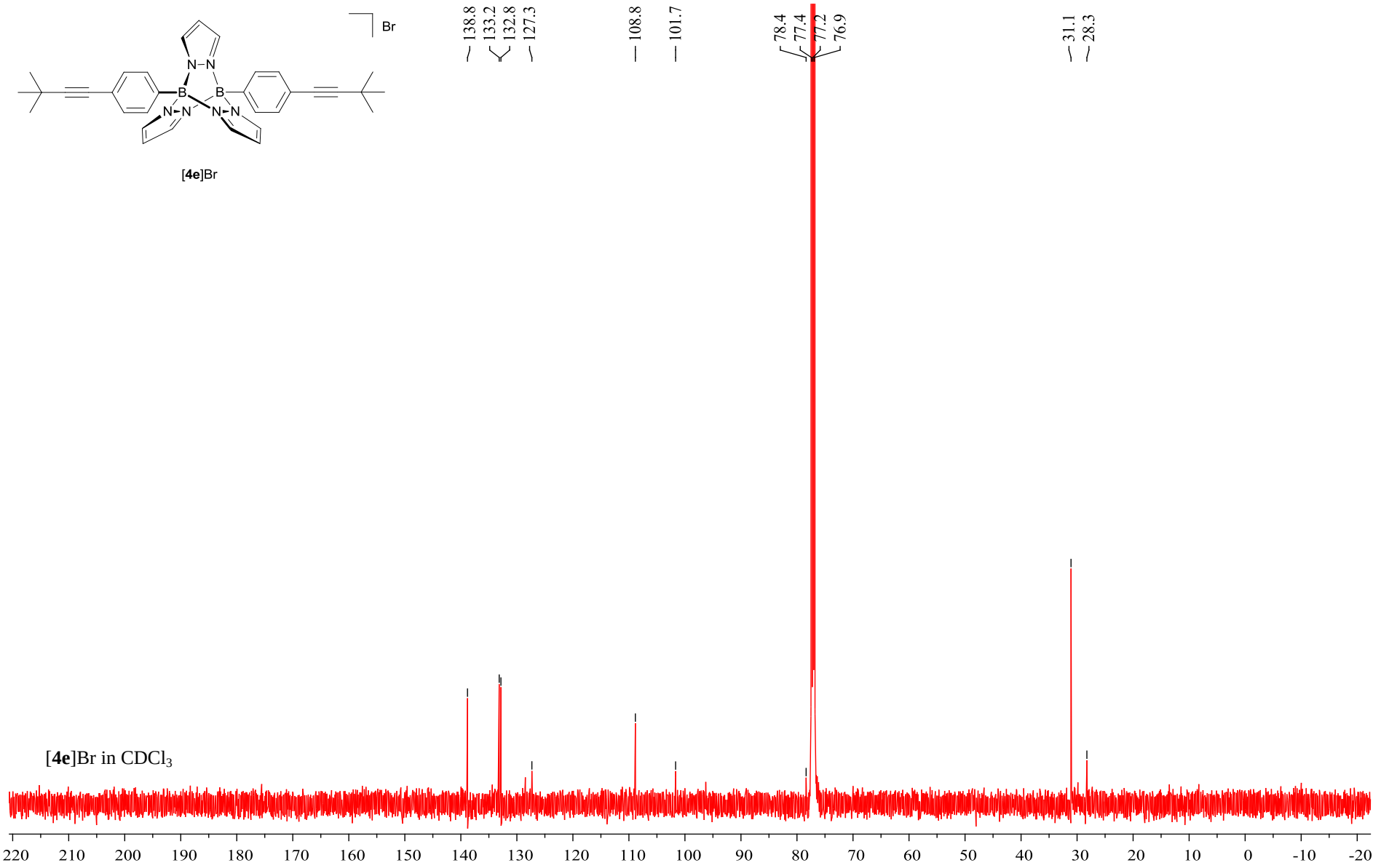
Br
[4e]Br
138.8
133.2
132.8
127.3
108.8
101.7
78.4
77.4
77.2
76.9
31.1
28.3
[4e]Br in CDCl3
220
210
200
190
180
170
160
150
140
130
120
110
100
90
80
70
60
50
40
30
20
10
0
-10
-20

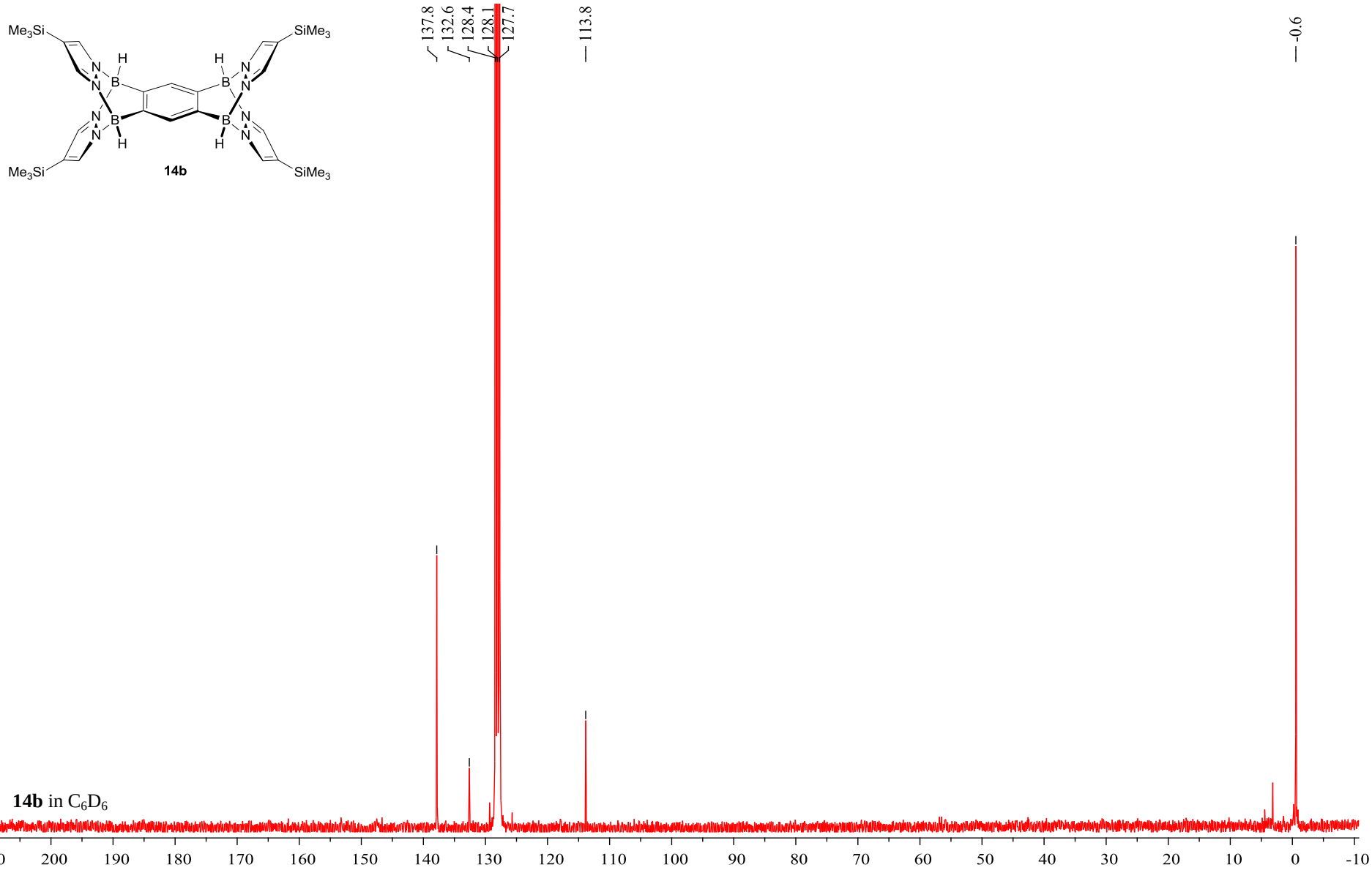
Me3Si
SiMe3
Me3Si
SiMe3
14b
137.8
132.6
128.4
128.1
127.7
113.8
-0.6
14b in C6D6
210
200
190
180
170
160
150
140
130
120
110
100
90
80
70
60
50
40
30
20
10
0
-10

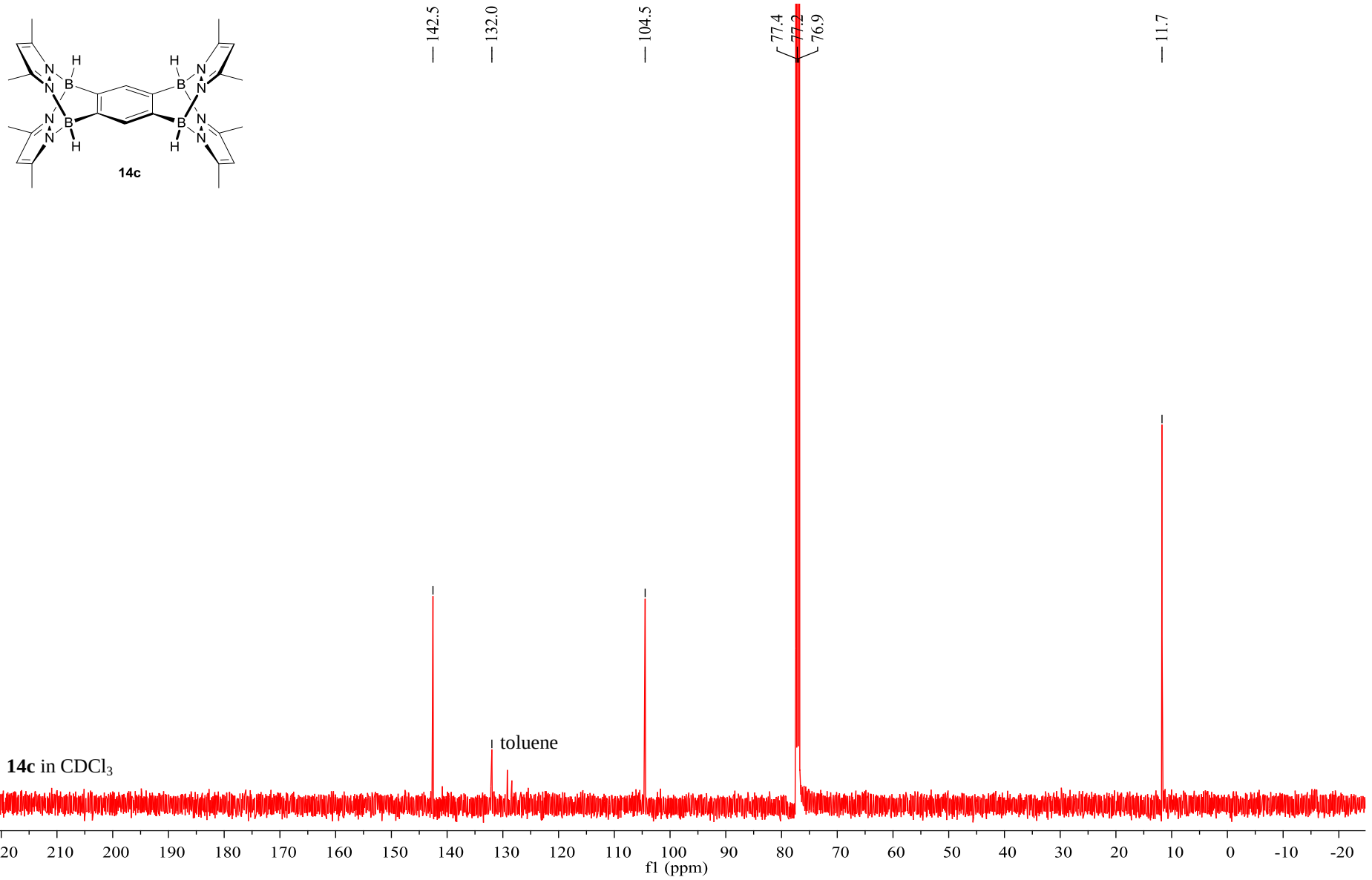
14c
142.5
132.0
104.5
77.4
77.2
76.9
11.7
toluene
14c in CDCl3
220 210 200 190 180 170 160 150 140 130 120 110 100 90 80 70 60 50 40 30 20 10 0 -10 -20
f1 (ppm)

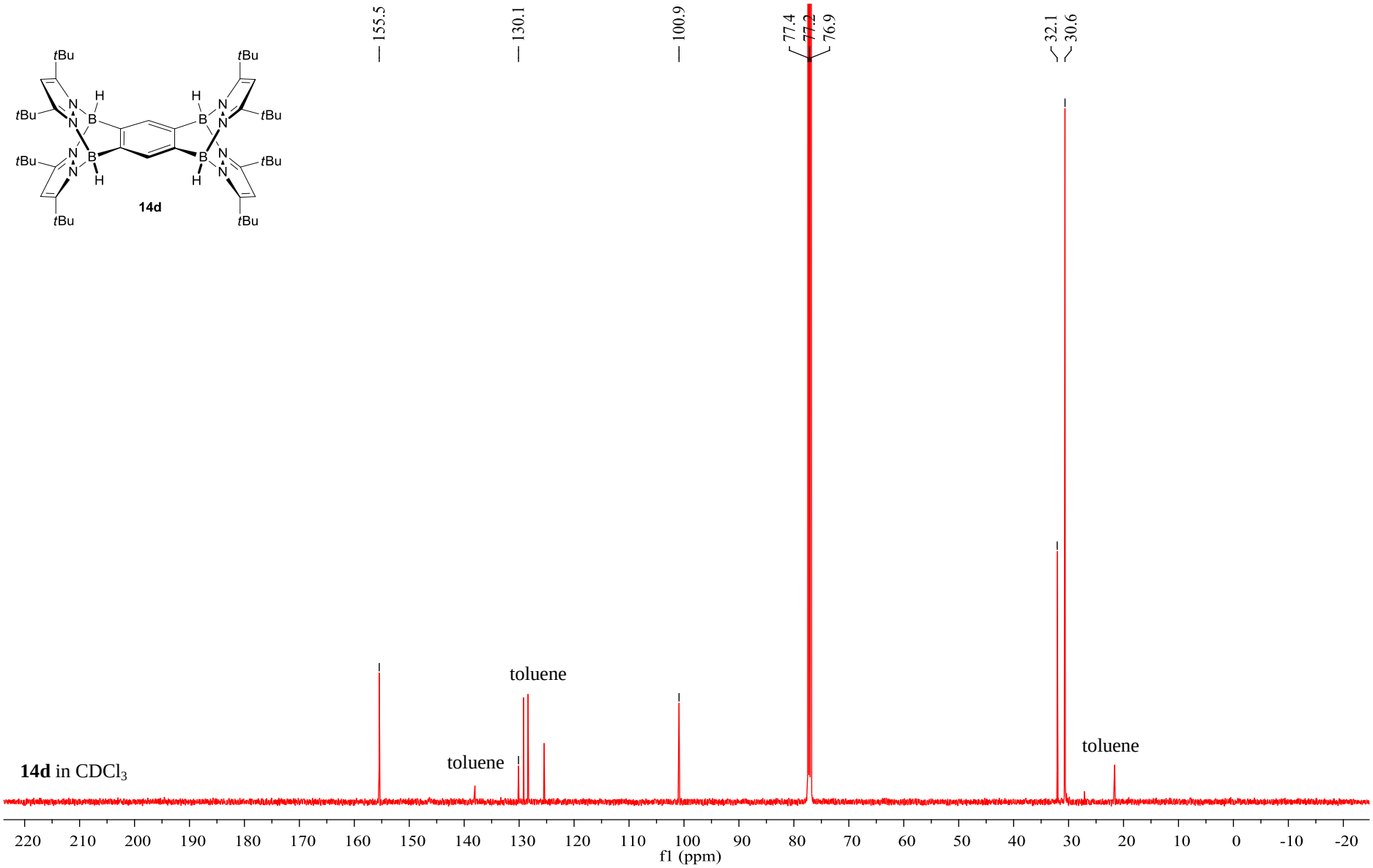
tBu
N
B
H
14d
155.5
130.1
100.9
77.4
77.2
76.9
32.1
30.6
toluene
toluene
toluene
14d in CDCl3
220 210 200 190 180 170 160 150 140 130 120 110 100 90 80 70 60 50 40 30 20 10 0 -10 -20
f1 (ppm)

3) Decomposition experiments of 3b, [4a]Br and [4b]Br in CD_3OD and [4d]Br in CH_3OH

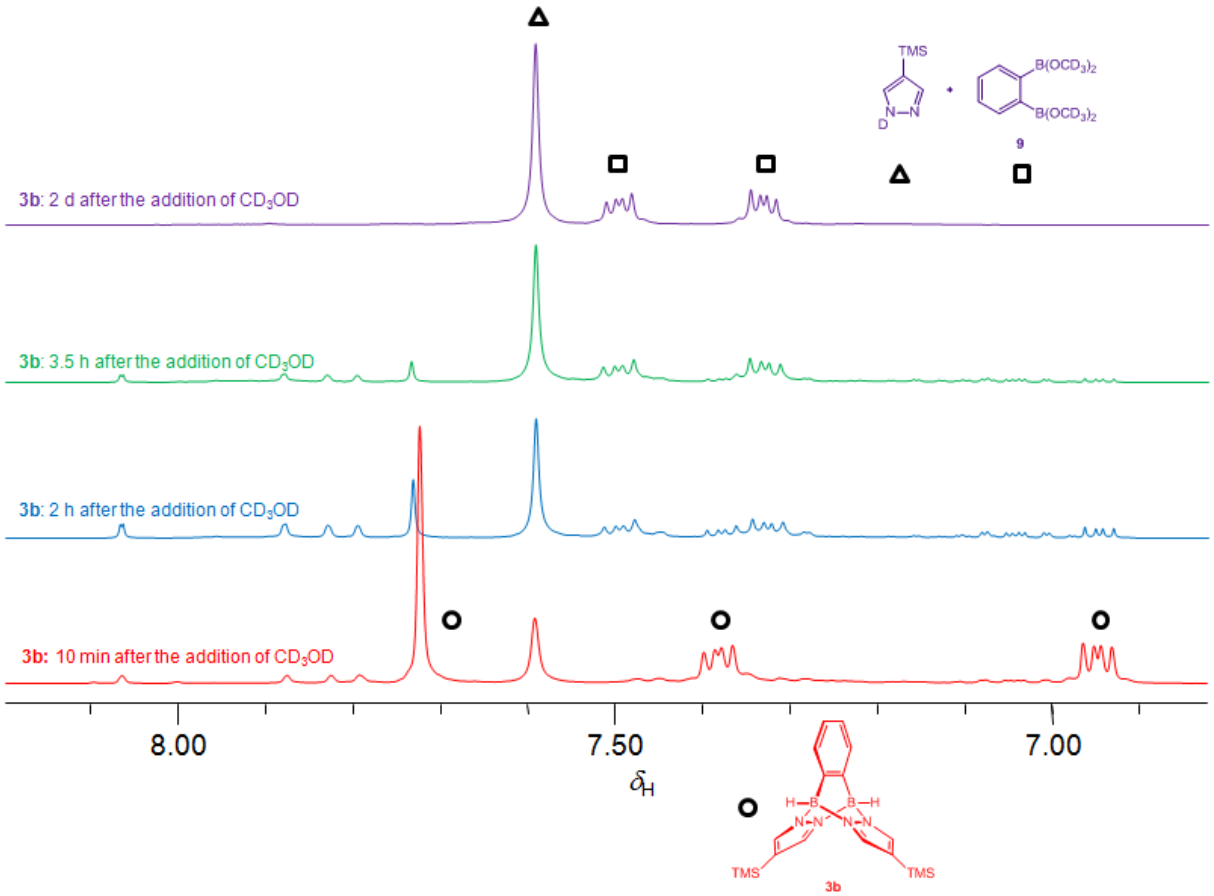

Figure 1S: ^{1}H NMR monitoring study of the slow decomposition of **3b** in non-dried, non-degassed CD_3OD (note: for simplicity reasons, the decomposition product has been drawn as CD_3OD ester, even though the corresponding boronic acid or mixed acid/ester species may well be present, too).

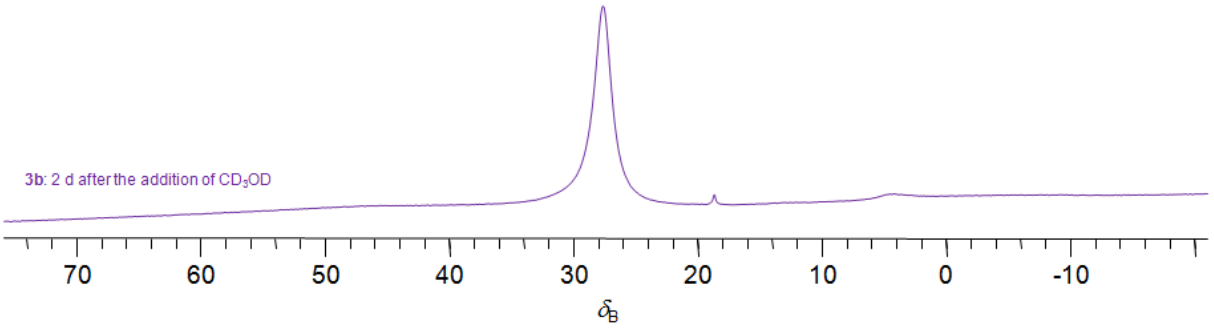

Figure 2S: $^{11}B\{^{1}H\}$ NMR spectrum of the decomposition mixture resulting from **3b** 2 d after the addition of CD_3OD.

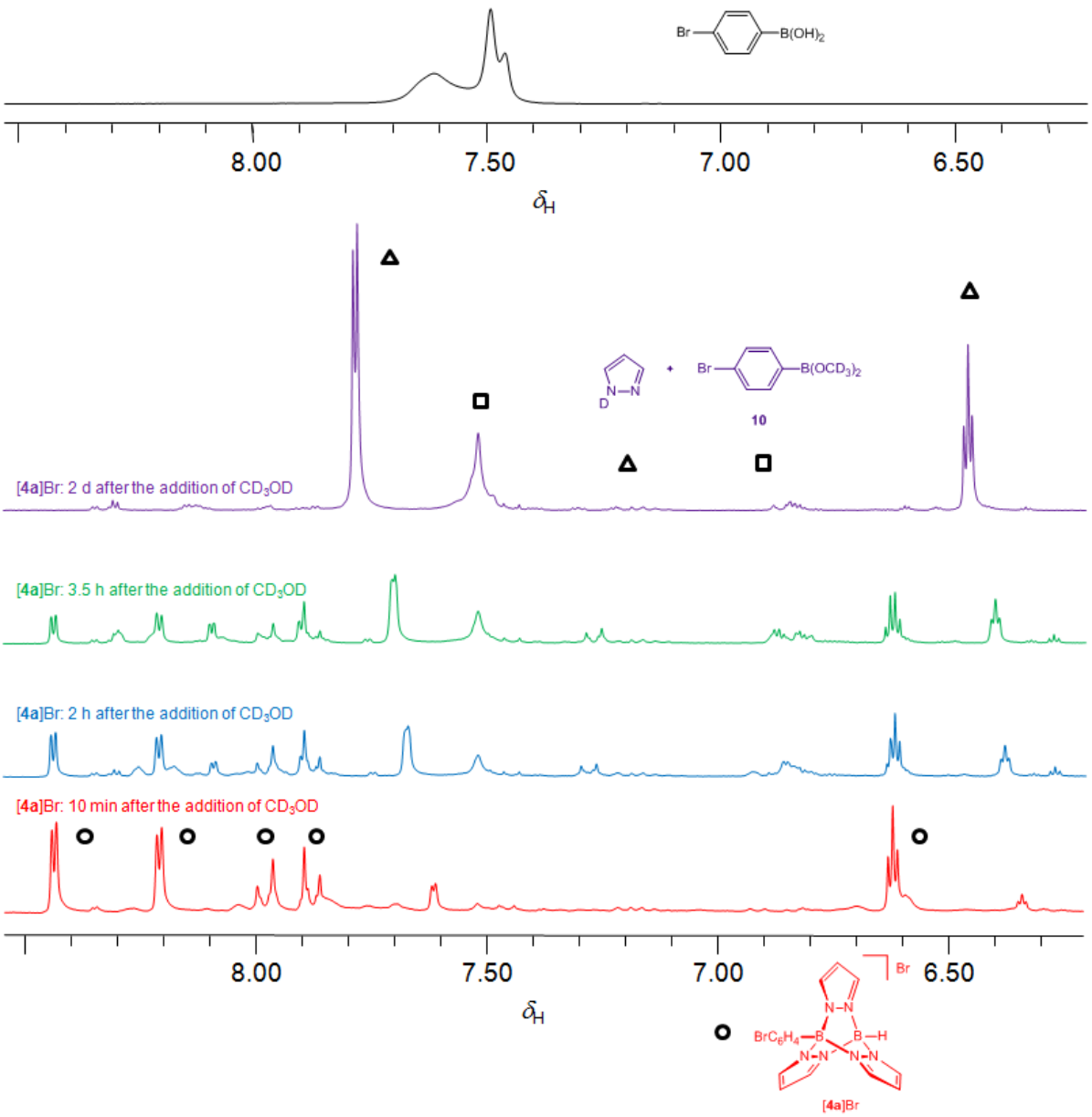

Figure 3S: ^{1}H NMR spectrum of *p*-$BrC_6H_4B(OH)_2$ in CD_3OD (top) and ^{1}H NMR monitoring study of the slow decomposition of [**4a**]Br in non-dried, non-degassed CD_3OD (bottom; note: for simplicity reasons, the decomposition product has been drawn as CD_3OD ester, even though the corresponding boronic acid or mixed acid/ester species may well be present, too).

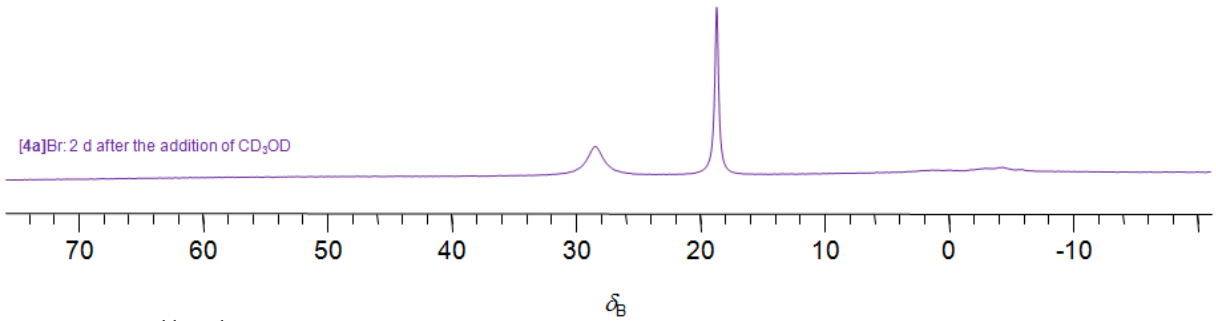

Figure 4S: $^{11}B\{^{1}H\}$ NMR spectrum of the decomposition mixture resulting from [**4a**]Br 2 d after the addition of CD_3OD.

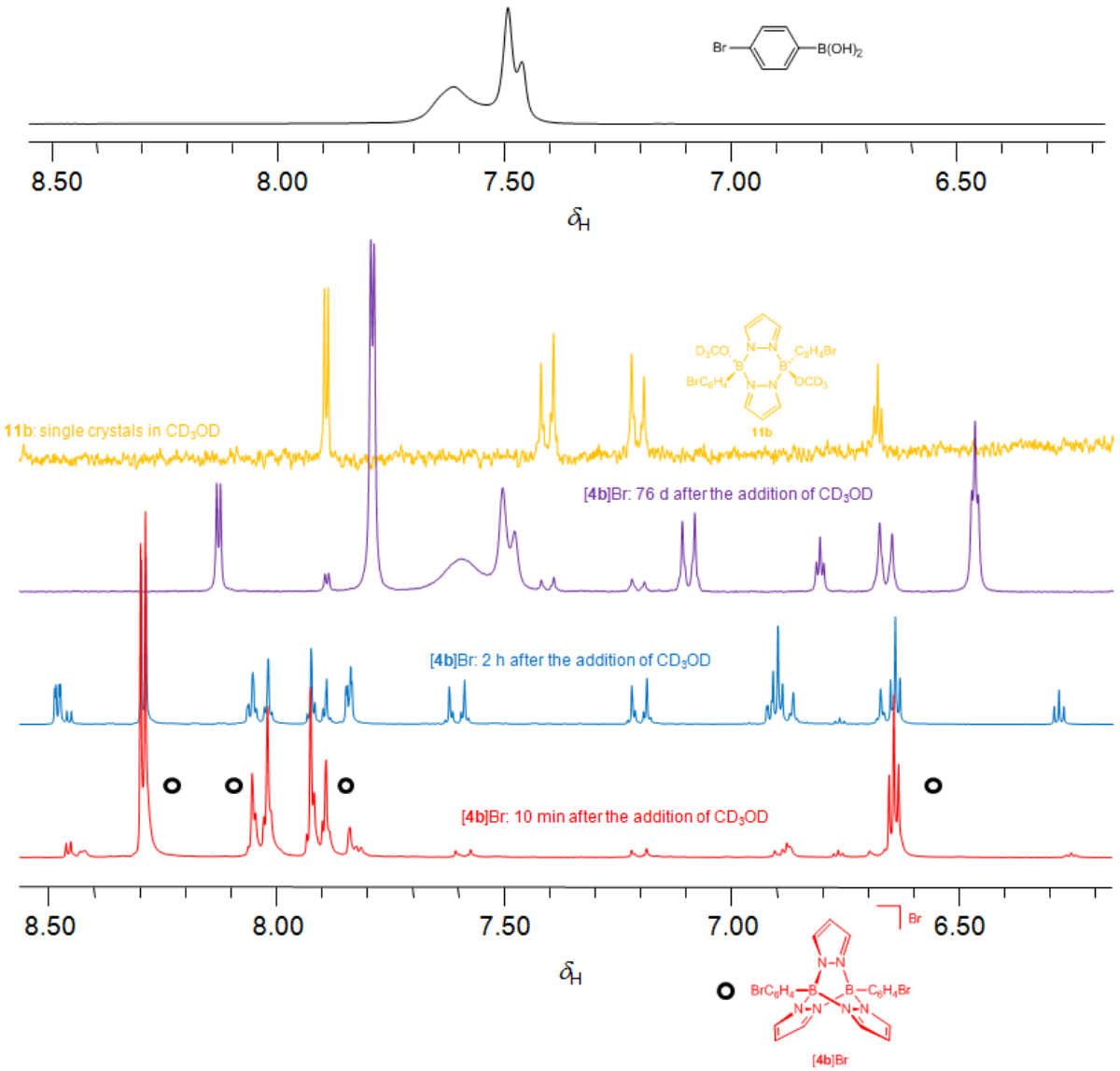

Figure 5S: ^{1}H NMR spectrum of *p*-$BrC_6H_4B(OH)_2$ in CD_3OD (top) and ^{1}H NMR monitoring study of the slow decomposition of [**4b**]Br in non-dried, non-degassed CD_3OD (bottom; note: for simplicity reasons, the decomposition products have been drawn as CD_3OD esters, even though the corresponding boronic acid or mixed acid/ester species may well be present, too).

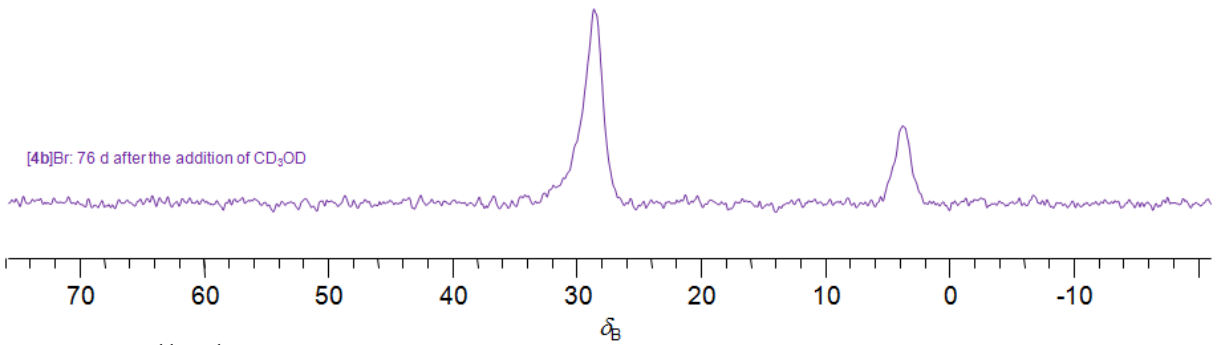

Figure 6S: ^{11}B{^{1}H} NMR spectrum of the decomposition mixture resulting from [**4b**]Br 76 d after the addition of CD_3OD.

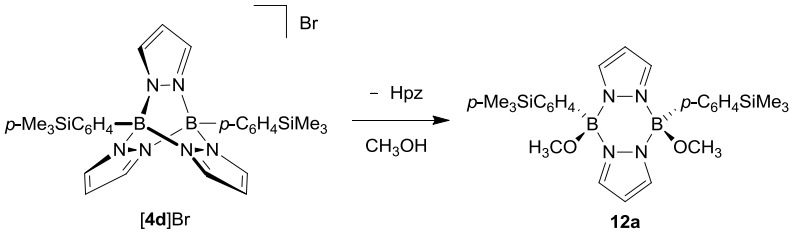

Scheme 2S: Decomposition of [**4d**]Br in CH_3OH leads to single crystals of **12a**.

4) X-ray crystal structure analyses of 3c, 3d, 3e, 3f·OEt_2 and 12a

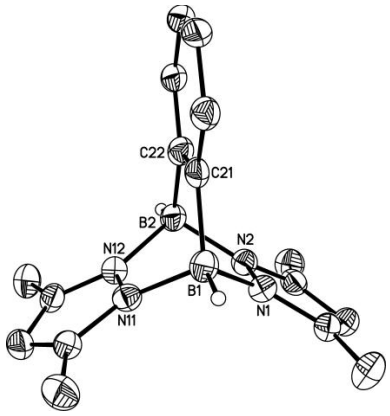

Figure 7S: Molecular structure of **3c** in the solid state. Hydrogen atoms except on boron have been omitted for clarity; displacement ellipsoids are drawn at the 50% probability level. Selected bond lengths (Å), atom···atom distance (Å), bond angles (°) and dihedral angles (°): B(1)−N(1) 1.577(4), B(1)−N(11) 1.573(4), B(1)−C(21) 1.611(4), B(2)−N(2) 1.585(4), B(2)−N(12) 1.580(4), B(2)−C(22) 1.607(4), B(1)···B(2) 2.687(5); N(1)−B(1)−N(11) 101.9(2), N(1)−B(1)−C(21) 105.8(2), N(11)−B(1)−C(21) 105.4(2), N(2)−B(2)−N(12) 102.2(2), N(2)−B(2)−C(22) 105.2(2), N(12)−B(2)−C(22) 105.3(2); N(1)B(1)N(11)//N(1)N(2)N(11)N(12) 48.9(2), N(2)B(2)N(12)//N(1)N(2)N(11)N(12) 47.6(2), pz(N(1))//C_6H_4 120.9(1), pz(N(11))//C_6H_4 119.0(1), pz(N(1))//pz(N(11)) 120.0(1); pz(N(X)) = pyrazolyl ring containing N(X).

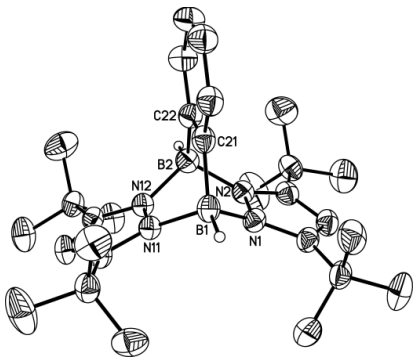

Figure 8S: Molecular structure of **3d** in the solid state. Hydrogen atoms except on boron have been omitted for clarity; displacement ellipsoids are drawn at the 50% probability level. Selected bond lengths (Å), atom···atom distance (Å), bond angles (°) and dihedral angles (°): B(1)−N(1) 1.599(3), B(1)−N(11) 1.583(3), B(1)−C(21) 1.586(3), B(2)−N(2) 1.578(3), B(2)−N(12) 1.594(3), B(2)−C(22) 1.607(3), B(1)···B(2) 2.655(3); N(1)−B(1)−N(11) 104.3(2),

N(1)−B(1)−C(21) 106.6(2), N(11)−B(1)−C(21) 104.8(2), N(2)−B(2)−N(12) 104.6(2), N(2)−B(2)−C(22) 105.3(2), N(12)−B(2)−C(22) 106.0(2); N(1)B(1)N(11)//N(1)N(2)N(11)N(12) 48.1(2), N(2)B(2)N(12)//N(1)N(2)N(11)N(12) 50.0(1), B(1)N(1)N(2)B(2)//B(1)N(11)N(12)B(2) 119.3(1), B(1)N(1)N(2)B(2)//B(1)C(21)C(22)B(2) 120.6(1), B(1)N(11)N(12)B(2)//B(1)C(21)C(22)B(2) 120.0(1), pz(N(1))//C_6H_4 108.3(1), pz(N(11))//C_6H_4 109.0(1), pz(N(1))//pz(N(11)) 141.3(1); pz(N(X)) = pyrazolyl ring containing N(X).

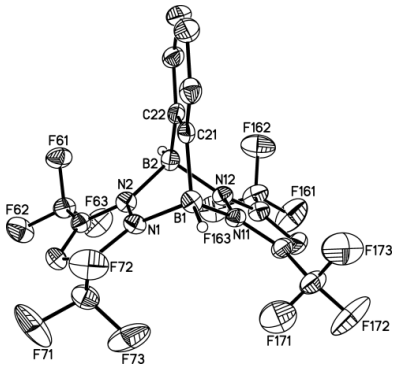

Figure 9S: Molecular structure of **3e** in the solid state. Hydrogen atoms except on boron have been omitted for clarity; displacement ellipsoids are drawn at the 50% probability level. Selected bond lengths (Å), atom···atom distance (Å), bond angles (°) and dihedral angles (°): B(1)−N(1) 1.594(4), B(1)−N(11) 1.609(4), B(1)−C(21) 1.603(4), B(2)−N(2) 1.599(4), B(2)−N(12) 1.586(4), B(2)−C(22) 1.587(5), B(1)···B(2) 2.707(5); N(1)−B(1)−N(11) 99.5(2), N(1)−B(1)−C(21) 104.8(2), N(11)−B(1)−C(21) 106.1(2), N(2)−B(2)−N(12) 99.8(2), N(2)−B(2)−C(22) 106.0(2), N(12)−B(2)−C(22) 105.8(2); N(1)B(1)N(11)//N(1)N(2)N(11)N(12) 49.1(2), N(2)B(2)N(12)//N(1)N(2)N(11)N(12) 48.8(2), pz(N(1))//C_6H_4 121.1(1), pz(N(11))//C_6H_4 122.6(1), pz(N(1))//pz(N(11)) 116.2(1); pz(N(X)) = pyrazolyl ring containing N(X).

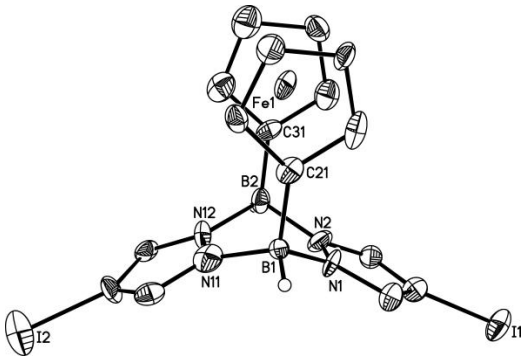

Figure 10S: Molecular structure of **3f**·OEt_2 in the solid state. Hydrogen atoms except on boron and the OEt_2 molecule have been omitted for clarity; displacement ellipsoids are drawn at the 50% probability level. The bond lengths and bond angles are not given due to poor crystallographic data, which lead to large error margins.

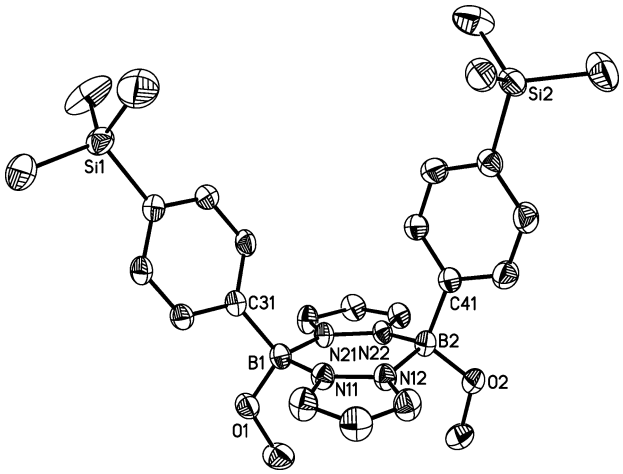

Figure 11S: Molecular structure of **12a** in the solid state. Hydrogen atoms have been omitted for clarity; displacement ellipsoids are drawn at the 50% probability level. Selected bond lengths (Å), atom···atom distances (Å), bond angles (°) and dihedral angles (°):
B(1)−O(1) 1.432(3), B(1)−N(11) 1.592(3), B(1)−N(21) 1.586(3), B(1)−C(31) 1.609(3), B(2)−O(2) 1.426(3), B(2)−N(12) 1.588(3), B(2)−N(22) 1.578(3), B(2)−C(41) 1.611(3), B(1)···B(2) 3.272(4), COG(Ar(C(31)))···COG(Ar(C(41))) 6.074; N(11)−B(1)−N(21) 104.9(2), N(12)−B(2)−N(22) 104.7(2); N(11)B(1)N(21)//N(12)B(2)N(22) 13.4(2), N(11)B(1)N(21)//N(11)N(12)N(21)N(22) 1.6(1), N(12)B(2)N(22)//N(11)N(12)N(21)N(22) 14.6(2), B(1)N(11)N(12)B(2)//B(1)N(21)N(22)B(2) 169.8(2), pz(N(11))//pz(N(21)) 171.4(1), Ar(C(31))//Ar(C(41)) 70.91(9); pz(N(X)) = pyrazolyl ring containing N(X); Ar(C(X)) = aryl ring containing C(X); COG(Ar(C(X))) = centroid of the aryl ring containing C(X).

Table 1S: Crystallographic Data for **3c**, **3d** and **3e**.

	3c	**3d**	**3e**
Formula	$C_{16}H_{20}B_2N_4$	$C_{28}H_{44}B_2N_4$	$C_{16}H_8B_2F_{12}N_4$
M_r	289.98	458.29	505.88
Colour, shape	Colourless, plate	Colourless, plate	Colourless, plate
T [K]	173(2)	173(2)	173(2)
Radiation, λ [Å]	MoKα, 0.71073	MoKα, 0.71073	MoKα, 0.71073
Crystal system	Triclinic	Monoclinic	Monoclinic
Space group	$P\bar{1}$	$P2_1/n$	$P2_1/n$
a [Å]	7.9633(10)	10.6013(7)	9.6394(8)
b [Å]	8.5150(11)	9.5489(6)	15.7965(13)
c [Å]	12.6954(17)	28.2614(17)	12.9452(12)
α [°]	71.470(10)	90	90
β [°]	81.729(11)	99.567(5)	101.491(7)
γ [°]	77.430(10)	90	90
V [Å^3]	794.05(19)	2821.1(3)	1931.6(3)
Z	2	4	4
D_{calcd} [g cm^{-3}]	1.213	1.079	1.740
F(000)	308	1000	1000
μ [mm^{-1}]	0.073	0.063	0.186
Crystal size [mm^3]	0.20 × 0.20 × 0.05	0.18 × 0.13 × 0.07	0.20 × 0.20 × 0.10
Rflns collected	8359	20700	29995
Independent rflns (R_{int})	2787 (0.0571)	5184 (0.0888)	3832 (0.1243)
Data/restraints/parameters	2787/0/211	5184/0/313	3832/0/315
GOF on F^2	1.239	0.923	1.155
R_1, wR_2 [$I > 2\sigma(I)$]	0.0648, 0.1601	0.0518, 0.1036	0.0755, 0.1265
R_1, wR_2 (all data)	0.0823, 0.1655	0.0990, 0.1171	0.1027, 0.1371
Largest diff. peak and hole [e Å^{-3}]	0.227, −0.256	0.209, −0.218	0.289, −0.256

Table 2S: Crystallographic Data for **3f**·OEt_2 and **12a**.

	3f·OEt_2	**12a**
Formula	$C_{16}H_{14}B_2FeI_2N_4$·$C_4H_{10}O$	$C_{26}H_{38}B_2N_4O_2Si_2$
M_r	667.70	516.40
Colour, shape	Yellow, needle	Colourless, needle
T [K]	173(2)	173(2)
Radiation, λ [Å]	MoKα, 0.71073	MoKα, 0.71073
Crystal system	Monoclinic	Monoclinic
Space group	$P2_1/c$	$P2_1/c$
a [Å]	11.061(3)	12.4434(10)
b [Å]	7.8312(14)	20.6663(13)
c [Å]	27.648(9)	12.4374(11)
α [°]	90	90
β [°]	98.73(2)	109.677(6)
γ [°]	90	90
V [Å^3]	2367.1(11)	3011.6(4)
Z	4	4
D_{calcd} [g cm^{-3}]	1.874	1.139
F(000)	1288	1104
μ [mm^{-1}]	3.265	0.146
Crystal size [mm^3]	0.15 × 0.01 × 0.01	0.52 × 0.10 × 0.10
Rflns collected	18238	20886
Independent rflns (R_{int})	4568 (0.2756)	5851 (0.0898)
Data/restraints/parameters	4568/162/271	5851/0/325
GOF on F^2	0.998	1.030
R_1, wR_2 [$I > 2\sigma(I)$]	0.1148, 0.1924	0.0777, 0.1489
R_1, wR_2 (all data)	0.2363, 0.2362	0.0994, 0.1584
Largest diff. peak and hole [e Å^{-3}]	1.165, −1.555	0.300, −0.326